The effects of multipath on a bathymetric synthetic aperture sonar using belief propagation

Michael Hayes and Philip Barclay
Acoustics Research Group,
Department of Electrical and Computer Engineering,
University of Canterbury, Christchurch, New Zealand
m.hayes@elec.canterbury.ac.nz

Abstract

This paper discusses the application of belief propagation to the reconstruction of bathymetric sonar images. Belief propagation is a powerful technique for probabilistic reasoning on Bayesian and Markov networks. It allows *a priori* information to be easily incorporated, in this case the expected seafloor height variation. We show that the algorithm works well without multipath interference but only a small improvement is obtained in the presence of multipath using a simple model. While a more sophisticated model incorporating multipath could be employed, the use of belief propagation would be computationally expensive.

Keywords: bathymetry, synthetic aperture sonar, belief propagation, multipath

1 Introduction

Swath bathymetric sidescan (SBS) is a sidescan imaging sonar technology that provides bathymetric information using two hydrophones configured as an interferometer. The time delay of an echo impinging on the hydrophones can be estimated to infer the angle of arrival of the incoming plane wave. While this technique has been successfully employed with radar, its application to sonar has been limited by sea-surface multipath and the footprint shift effect.

Standard interferometric phase techniques for estimating the angle of arrival assume that there is only a single plane wave incident upon the hydrophones at any instant [1]. Unfortunately in a shallow water environment, echoes from the seafloor are also scattered by the sea-surface; a phenomenon known as multipath [2]. Thus at any instant there can be two or more echo signals measured; the direct path signal plus the interfering indirect path signals. Moreover, some seafloor geometries, such as a proud object, can produce multiple echoes with the same delay. These multiple echoes interfere and cannot be resolved by a two hydrophone interferometer. The resulting angle of arrival estimate varies according to the relative phase and strength of the interfering signals [3, 4] and can lie well outside the range of incoming angles [5].

The footprint shift effect reduces the coherence between the received signals and thus results in noisy angle of arrival estimates [6]. The effect is simply due to the misregistration between the echoes received by the hydrophones. The misregistration can be compensated by time shifting of the echoes but this requires an accurate estimate of the seafloor height. Iterative schemes have been proposed to deal with this problem [6, 7]. An alternative technique is to use a probabilistic approach to estimate the most likely scattering surface. A promising approach is to generate a compatability metric for all possible scattering voxels and to employ belief propagation to find the most likely solution [8]. Priors for the expected surface geometry can be easily added so that a maximum *a posteriori* (MAP) estimate of the scattering surface can be found.

In this paper we examine the effects of sea-surface multipath on the reconstruction of seafloor bathymetry using belief propagation techniques. We start with developing a simple model for the echo signals received by a hydrophone array for an active sonar and then extend the model in Section 3 to consider sea-surface multipath. Bathymetric reconstruction using back-projection with belief propagation is presented in Section 4, followed by results of simulations in Section 5 and a discussion in Section 6.

2 Echo signal model

Consider a linear array of H hydrophones vertically spaced by d. After pulse-compression the measured baseband signal from the h^{th} hydrophone can be modelled (ignoring the angular dependence of the beam patterns) using

$$d_h(t) = \sum_{i=1}^{I} a_i ss\left(t-\tau_{h,i}\right)\exp\left(-j2\pi f_0\tau_{h,i}\right) + n_h(t). \tag{1}$$

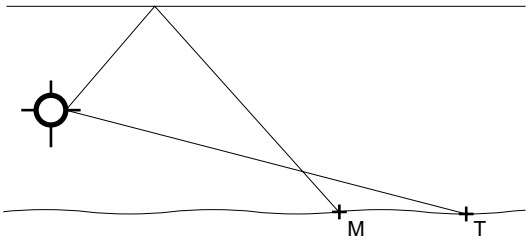

Figure 1: Sonar geometry showing the direct path and a sea-surface reflected multipath.

where $ss(t)$ is the autocorrelation of the transmitted signal, f_0 is the centre frequency, a_i is a complex amplitude (incorporating spreading losses and assuming matched hydrophones) for the i^{th} scatterer, $\tau_{h,i}$ is the propagation delay for the i^{th} scatterer, and $n_h(t)$ represents any noise. The propagation delay depends on the range r_i between the projector and the i^{th} scatterer and the range $r_{h,i}$ between the the i^{th} scatterer to the h^{th} hydrophone,

$$\tau_{h,i} = \frac{r_i + r_{h,i}}{c}. \tag{2}$$

where c is the speed of acoustic propagation. If the scatterer is in the far-field of the hydrophone array, the ranges can be approximated by

$$r_{h,i} \approx r_{1,i} + (h-1)d\sin\psi_i, \tag{3}$$

and so the propagation delays are

$$\tau_{h,i} = \tau_{1,i} + \Delta\tau_{h,i}, \tag{4}$$

where the differential propagation delays are

$$\Delta\tau_{h,i} \approx (h-1)(d/c)\sin\psi_i = (h-1)\Delta\tau_i. \tag{5}$$

Using this approximation, (1) becomes

$$\begin{aligned} d_h(t) \approx \sum_{i=1}^{I} a_i ss\left(t - \tau_{1,i} - \Delta\tau_{h,i}\right) \\ \times \exp\left(-j2\pi f_0(h-1)\Delta\tau_i\right) + n_h(t). \end{aligned} \tag{6}$$

where the additional phase shift $2\pi f_0\tau_{1,i}$ has been incorporated into a_i. When the signal is narrowband, the shift of the envelope can be ignored, so

$$d_h(t) \approx \sum_{i=1}^{I} a_i ss\left(t - \tau_{1,i}\right)\exp\left(-j2\pi f_0(h-1)\Delta\tau_i\right) + n_h(t). \tag{7}$$

3 Sea-surface multipath

Consider a point T on the seafloor at $(x_1, 0, z_1)$ producing an echo measured by a hydrophone at $(0, 0, z_h)$. From Figure 1, the range and angle of arrival are respectively,

$$r_{h,1} = \sqrt{x_1^2 + (z_h - z_1)^2}, \tag{8}$$

$$\psi_{h,1} = \tan^{-1}\frac{z_h - z_1}{x_1}. \tag{9}$$

Here $r_{h,1}$ is the range from the scatterer to the h^{th} hydrophone assuming a direct straight path. Now also consider a second point M at $(x_2, 0, z_2)$ on the seafloor. If the sea-surface is smooth compared to the sonar wavelength then it will act as a mirror and the scatterer will also appear above the sea-surface at $(x_2, 0, -z_2)$. This is known as the Lloyd's mirror effect. An echo from the scatterer reflected from the sea-surface will take a longer indirect path to reach the sonar and will have a different angle of arrival:

$$r'_{h,2} = \sqrt{x_2^2 + (z_h + z_2)^2}, \tag{10}$$

$$\psi'_{h,2} = \tan^{-1}\frac{(z_h + z_2)}{x_2}. \tag{11}$$

These multipath echoes generate ghost artefacts masking other scatterers and corrupting bathymetry estimates.

There are also other indirect paths involving additional seafloor and sea-surface reflections. Except in 'bright' acoustic environments, these additional indirect echoes have less energy than the single reflection sea-surface reflected echoes.

Of interest is the portion of the echo signal where the direct echo from scatterer 1 overlaps with the indirect echo from scatterer 2. Assuming that the hydrophone array has a small vertical extent compared to the range resolution of the sonar, the shifts of the echo envelope are similar and so the echo signal in the range bin of interest has the form

$$\begin{aligned} d_{h,n} \approx a_1 \exp\left(-j2\pi f_0(h-1)\Delta\tau_1\right) \\ + a'_2 \exp\left(-j2\pi f_0(h-1)\Delta\tau_{2'}\right) + n_{h,n}. \end{aligned} \tag{12}$$

4 Belief propagation

Belief propagation is an efficient technique based on local message passing that can be used to find the most likely state of a system given any available evidence. By appropriately modelling the system, this approach can be applied to bathymetric data to produce an improved estimate of the sea floor height [8]. Although originally proposed by Pearl [9] for performing probabilistic reasoning on Bayesian networks, the technique has since been successfully applied to the stereo imaging field [10, 11, 12]. In most of this work, the system is modelled as a hidden pairwise Markov Random Field (MRF) [13]. Belief propagation is then applied to this model, acting as a statistical filter to find the most likely surface, given initial evidence for each voxel and the expected variation between neighbouring points.

Belief propagation iterates to find the most likely surface within the reconstruction volume given *a priori* information of the expected surface and the evidence for each voxel being a surface point. This *a priori* information is expressed in terms of neighbourhood function that describes the expected relationship between voxels. The evidence of a voxel being a surface point is estimated from the consistency of the back-projected images from each hydrophone.

To apply belief propagation to bathymetric data, the scene is represented as a connected 3D array of nodes, whose values correspond to the surface heights. Associated with each node are a set of beliefs which give a measure how likely the surface is at any particular height. The objective is to calculate these beliefs as accurately as possible, by propagating the original belief estimates throughout the network.

The evidence estimates are calculated by back-projecting the image data for each hydrophone over circular arcs into the reconstruction volume (compare this with stereo vision where the camera data is back-projected along rays [14]). These arcs have a radius corresponding to the range of each image pixel. The points in the volume where the measured data is consistent is likely to correspond to the position of a scatterer. The evidence for each voxel is calculated using

$$E = \exp\left(-\pi \frac{\sigma_q^2}{\sigma_n^2}\right), \tag{13}$$

where σ_n^2 is the estimated noise variance, σ_q^2 is the backprojected echo variance at each voxel,

$$\sigma_q^2 = \frac{1}{H}\sum_{h=1}^{H} |q_h - \overline{q}|^2, \tag{14}$$

q_h is the backprojected echo value for hydrophone h, and $\overline{q}$ is the mean backprojected echo value,

$$\overline{q} = \frac{1}{H}\sum_{h=1}^{H} q_h. \tag{15}$$

5 Results

To demonstrate the algorithms, the echoes received by three hydrophones from a rough seafloor were simulated for a single ping using the parameters of the KiwiSAS sonar [15]. The salient parameters include a centre frequency $f_0 = 30\,\text{kHz}$, three hydrophones spaced by $d = 75\,\text{mm}$, a sonar depth $z_s = 5\,\text{m}$, and a mean water depth of 10 m. A sinusoidal seafloor profile with a 2 m peak-peak variation and a 5 mm rms Gaussian roughness was represented using a point scatterer model [16].

Fig. 2(a) shows an example of a bathymetric image reconstructed using two hydrophones as a phase interferometer. The height estimates are noisy primarily due to the misregistration caused by the footprint shift effect [6]. Fig. 2(b) shows the evidence image calculated using (13). Note that the evidence is greatest at the position of the seafloor surface and that there are a number of artefacts. These are primarily due to grating lobes resulting from the hydrophone separation being greater than half the wavelength. Also note that the evidence is the same at all angles for ranges shorter than the sonar altitude above the seafloor. This is reasonable since all angles are equally likely when there is no information.

The computed beliefs after two and twenty iterations of belief propagation as shown in Fig. 2(c) and (e) and the corresponding most likely surface profile is shown in Fig. 2(d) and (f). Note how the artefacts are removed and how the most likely surface has converged after twenty iterations. Also note that the most likely surface height has become less sinusoidal. This is due to the simple choice of neighbourhood function to describe the expected surface height variation.

Fig. 3 shows the equivalent images to Fig. 2 but with additive multipath from a smooth sea-surface. Note how reasonable height estimates are obtained out to about 15 m. This is to be expected since in this region there is no multipath component. After about 30 m the evidence estimates are invalid since they are computed assuming a single scattering point in each range bin. While the belief propagation algorithm generates a smoother height estimate, the results are invalid due to the invalid initial evidence estimates.

6 Discussion

While the use of bathymetric reconstruction using belief propagation can remove some sea-surface multipath on the basis of surface continuity, it does not discriminate between a direct and indirect path echo. Apart from some blurring of the indirect path echoes due to motion of the sea-surface over the synthetic aperture formation time, the only difference between an indirect path echo and a direct path echo is the angle of arrival.

The failure of the technique is not surprising since it is using an incorrect model. Currently only the angle of arrival of the direct path echo is estimated but this is corrupted by the multipath echo. However, to model the multipath component it is necessary to estimate the angle of arrival of the multipath and the complex amplitudes of the direct and multipath echoes. In principle, belief propagation could be used to find the most likely solution but this is not computationally practicable. This is because evidence needs to be determined over a six dimensional space for each range bin rather than a one dimensional space for each range bin. Fur-

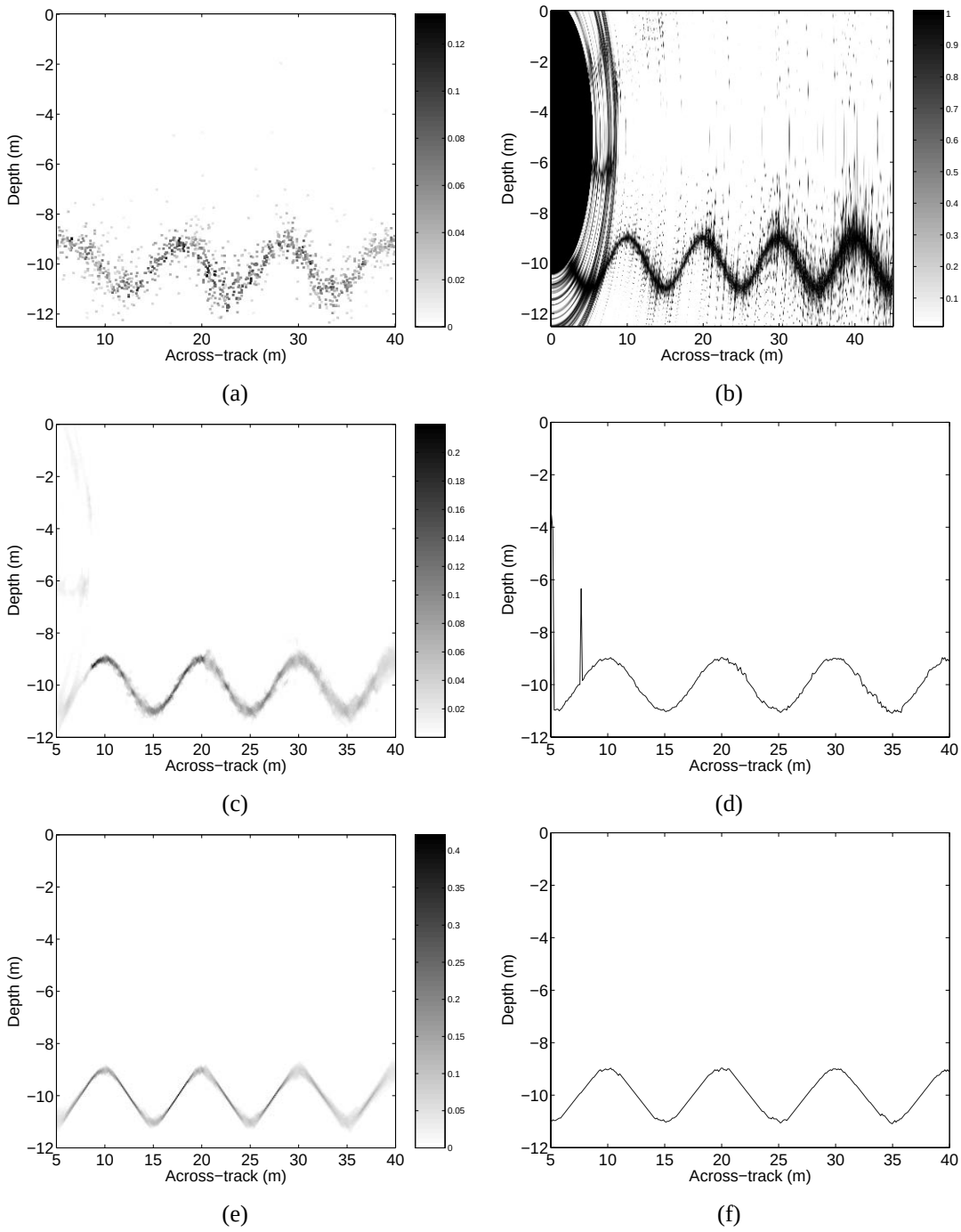

Figure 2: Reconstructed images of data without multipath: (a) reconstructed bathymetric image using a pair of hydrophones as an interferometer with no footprint shift compensation, (b) initial evidence provided to the belief propagation algorithm, (c) beliefs after two iterations of belief propagation, (d) most probable height estimate after two iterations of belief propagation, (e) beliefs after twenty iterations of belief propagation, (f) most probable height estimate after twenty iterations of belief propagation.

thermore, it is likely that an even larger search space would be required to deal with multiple bounce multipath (where multipath echoes are also re- reflected from the seafloor).

An alternate approach is to estimate the multipath directly. Techniques have been proposed for resolving the multiple angles of arrival using a small vertical array of hydrophones, for example, Computed Angle-of-Arrival Transient Imaging (CAATI) [5] and Coherent Source Direction Estimation (CSDE) [17]. For fully

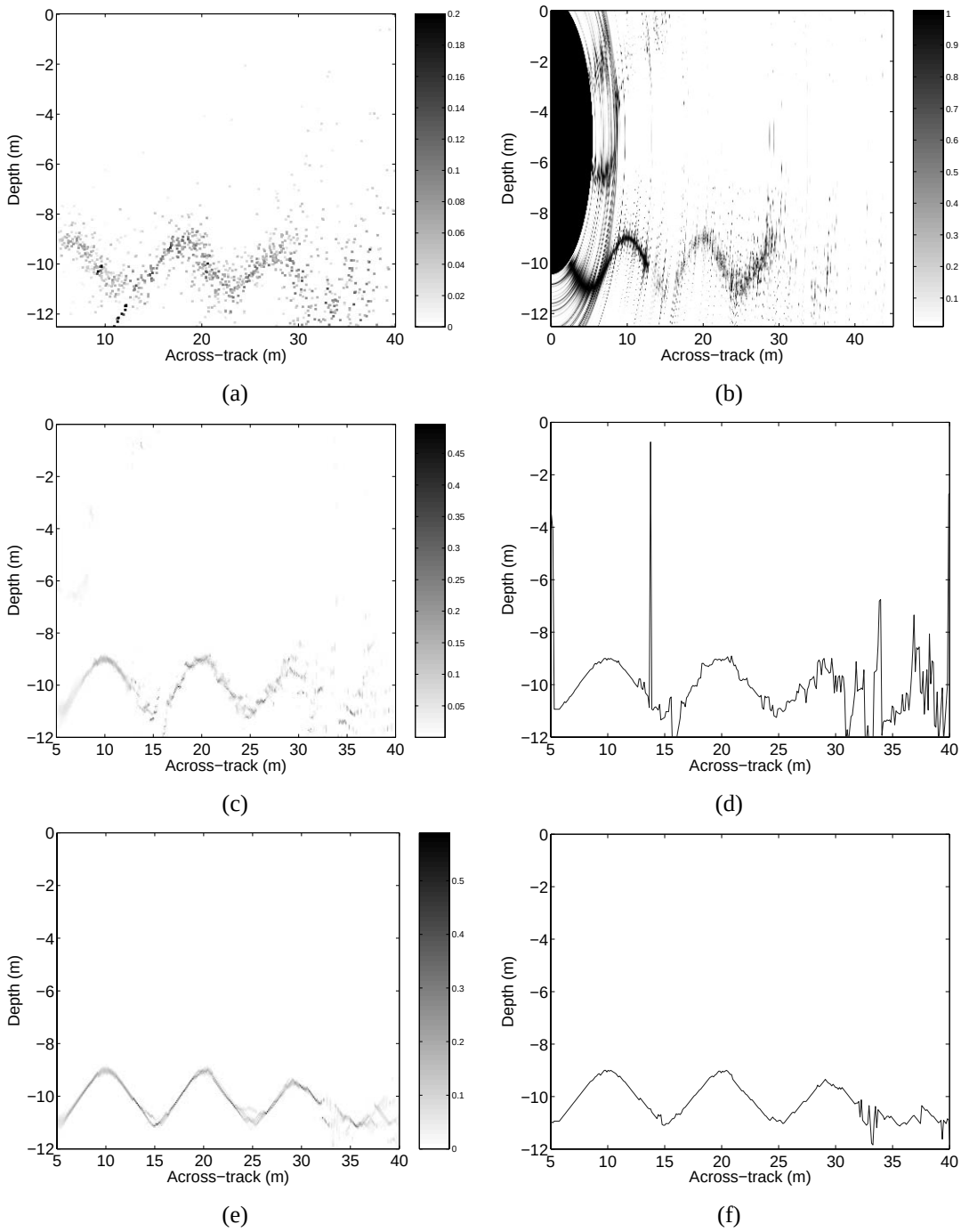

Figure 3: Reconstructed images of data with simulated multipath: (a) reconstructed bathymetric image using a pair of hydrophones as an interferometer with no footprint shift compensation, (b) initial evidence provided to the belief propagation algorithm, (c) beliefs after two iterations of belief propagation, (d) most probable height estimate after two iterations of belief propagation, (e) beliefs after twenty iterations of belief propagation, (f) most probable height estimate after twenty iterations of belief propagation.

uncorrelated arrivals CAATI with H hydrophones can resolve $H-1$ arrivals or $H/2$ fully coherent arrivals while CSDE is claimed to resolve 2 coherent arrivals with $H=3$ hydrophones. However, both these techniques are only applicable to narrowband systems.

The CAATI algorithm determines the six unknowns at each range bin (the complex amplitudes a_1 and a_2' and the angles ψ_1 and ψ_2') by solving the null steering equation

$$\sum_{h=1}^{H} w_h d_h = 0, \tag{16}$$

for the unknown weights w_h in a least squares sense [5].

A better approach would be to maximise the *posterior* probability using prior information such as the expected angles of arrival of the direct and multipath echoes based on the expected continuity of the seafloor. While the gradients can be calculated to speed up the search, it is more computationally expensive.

7 Conclusion

In this paper we have presented some preliminary results assessing the effect of sea-surface multipath on bathymetric reconstruction using back-projection with belief propagation. While some rejection of the multipath is shown, the model employed is inadequate to properly suppress its effect. However, extending the model to incorporate multipath does not appear to be computationally feasible using belief propagation.

References

[1] Mohammed A. Masnadi-Shirazi, Christian de Moustier, Pierre Cervenka, and Stanley H. Zisk. Differential phase estimation with the SeaMARC II bathymetric sidescan sonar system. *IEEE J. Oc. Eng.*, 17(3):239–251, July 1992.

[2] J. F. Dix and R. F. Palmer. Study of the relative sonar performance of incoherent and coherent processing against echo fading in shallow water. *Proc. IEE*, 131, Part F(3):308–314, June 1984.

[3] R. B. Dybdal. Monopulse resolution of interferometric ambiguities. *IEEE Trans. on Aerospace and Electronic Systems*, AES-22(2):177–183, March 1986.

[4] I. E. Kliger and C. F. Olenberger. Multiple target effects on monopulse signal processing. *IEEE Trans. on Aerospace and Electronic Systems*, AES-11(5):795–803, September 1975.

[5] Paul H. Kraeutner and John S. Bird. Beyond interferometry, resolving multiple angles-of-arrival in swath bathymetric imaging. In *IEEE Oceans '97 Conference Proceedings*, pages 37–45, 1997.

[6] P. J. Barclay, M. P. Hayes, and P. T. Gough. Bathymetry reconstruction for a free-towed synthetic aperture sonar. In *Proceedings of the World Congress on Ultrasonics*, September 2003. CDROM.

[7] S. M. Banks, H. D. Griffiths, and T. J. Sutton. A technique for interferometric synthetic aperture sonar image processing. In *London Communications Symposium*, September 2001.

[8] P. J. Barclay, M. P. Hayes, and P. T. Gough. Reconstructing seafloor bathymetry with a multi-frequency, multi-channel broadband InSAS using belief propagation. In *Oceans 2003*, pages 2149–2155. IEEE, MTS, September 2003.

[9] J. Pearl. *Probabilistic reasoning in intelligent systems: networks of plausible inference*. Morgan Kaufmann Publishers, San Mateo, Calif., 2nd revised edition, 1988.

[10] J. Sun, H. Y. Shum, and N. N. Zheng. Stereo matching using belief propagation. In *Proceedings of the European Conference on Computer Vision*, volume 2, pages 510–524, Copenhagen, Denmark, May 2002.

[11] N. Petrovic, I. Cohen, B. J. Frey, R. Koetter, and T. S. Huang. Enforcing integrability for surface reconstruction algorithms using belief propagation in graphical models. In *Computer Vision and Pattern Recognition, 2001*, volume 1, pages I743–I748. IEEE, 2001.

[12] A. Minagawa, K. Uda, and N. Tagawa. Region extraction based on belief propagation for gaussian model. In *Pattern Recognition, 2002 Proceedings*, volume 2, pages 507–510. IEEE, 2002.

[13] J. S. Yedidia, W. T. Freeman, and Y. Weiss. Understanding belief propagation and its generalizations. In *2001 International Joint Conference on Artificial Intelligence*, August 2001.

[14] C. J. Forne and M. P. Hayes. A maximum likelihood approach to reconstructing scenes from photometric images. In *IVCNZ2001, Image and Vision Computing New Zealand 2001*, pages 151–156, University of Otago, Dunedin, New Zealand, November 2001.

[15] M. P. Hayes, P. J. Barclay, P. T. Gough, and H. J. Callow. Test results from a multi-frequency bathymetric synthetic aperture sonar. In *OCEANS2001*, pages 1682–1687, Honolulu, Hawaii, November 2001.

[16] A. J. Hunter, M. P. Hayes, and P. T. Gough. Simulation of multiple-receiver, broadband interferometric SAS imagery. In *OCEANS 2003*, San Diego, USA, September 2003. IEEE. CDROM.

[17] Wen Xu and W. Kenneth Stewart. Coherent source direction fot[sic] three-row bathymetric sidescan sonars. In *OCEANS 1999*, volume 1, pages 299–304, 1999.